

K-shell x-ray production cross sections of selected elements from Ti to Y for 0.5- to 2.5-MeV alpha-particle bombardment*

F. D. McDaniel, Tom J. Gray, and R. K. Gardner

Department of Physics, North Texas State University, Denton, Texas 76203

(Received 18 November 1974)

K-shell x-ray production cross sections and $K\beta/K\alpha$ ratios have been measured for thin targets of Ti, V, Cr, Fe, Ni, Cu, Zn, Ga, As, Se, Rb, Sr, and Y for 0.5- to 2.5-MeV alpha particles. The experimental values are compared to the nonrelativistic plane-wave Born approximation (PWBA), the binary-encounter approximation, and the PWBA with binding energy and Coulomb deflection corrections. The PWBA with corrections provides the best agreement with the experimental cross sections.

I. INTRODUCTION

Since the development of high-resolution x-ray detectors, considerable progress has been made in the study of inner-shell ionization induced by light-ion bombardment. Early work has been summarized in a number of excellent review articles by Garcia, Fortner, and Kavanagh,¹ Lin, Duggan, and Carlton,² and Rutledge and Watson.³

The practical applications of characteristic x-ray analysis in ion-implantation⁴ and trace analysis⁵⁻⁷ are well known. For these applications precise x-ray cross sections are needed. While considerable work has been reported for hydrogen-ion projectiles¹⁻¹³ there is a marked absence of α -particle data between 0.5 and 2.5 MeV. Lin, Duggan, and Carlton^{2,14} have presented α -particle cross sections for incident energies from 2.0 to 12.0 MeV in 1.0-MeV steps for Ca, Ti, Fe, Co, Ni, Zn, Cu, and Ag. Other α -particle work has been limited to energies less than 0.2 MeV¹⁵ or to higher energies of 30–80 MeV.¹⁶

Two primary theoretical approaches, which have been employed to describe direct Coulomb ionization of inner-shell electrons, are the quantum-mechanical plane-wave Born approximation (PWBA) and the semiclassical binary encounter approximation (BEA).

The PWBA treatment of the incident projectile as a plane wave has been described in a review article by Merzbacher and Lewis.¹⁷ The PWBA involves a number of simplifying assumptions. The electronic states are described by nonrelativistic hydrogenic wave functions which are undisturbed by the Coulomb interaction between the incident projectile and the target electrons. The screening of the nuclear charge of the target atom is approximated by replacing the nuclear charge Z by an effective Z_e . Results of the calculations have been tabulated by Khandelwal, Choi, and Merzbacher.¹⁸ While the PWBA has been shown to provide good estimates of the x-ray cross sec-

tions for energies greater than a few MeV, it overpredicts the cross sections at lower energies.^{2,19}

The BEA, which has been developed by Garcia and co-workers,²⁰⁻²² assumes that the ionization is produced by a direct energy exchange between the incident projectile and an inner electron. The BEA results have been found to compare more favorably than the PWBA with the experimental cross sections at low energies.²

Corrections have been made to the PWBA by Basbas, Brandt, and Laubert for Coulomb deflection of the incident projectile by the nuclear charge of the target and for increasing binding of the target electrons due to the penetration of the K shell by the projectile.²³ The PWBA corrected for binding and Coulomb deflection (PWBABC) provides the best estimate of the magnitude of the experimental cross section.¹⁹

The present thin-target results were taken for the elements Ti, V, Cr, Fe, Ni, Cu, Zn, Ga, As, Se, Rb, Sr, and Y. The K -shell x-ray-production cross sections and $K\beta/K\alpha$ ratios were determined. The present results will be compared to other thin-target α -particle results and with the predictions of the PWBA, the PWBA with binding-energy and Coulomb-deflection corrections, and the BEA. Preliminary portions of the data have been reported earlier.²⁴

II. EXPERIMENTAL PROCEDURES

Data were taken with the 2.5-MeV Van de Graaff accelerator in the Regional Nuclear Physics Laboratory at North Texas State Univ. The experimental apparatus has been described in detail earlier^{8,12} and will only be discussed briefly.

A 100–300-nA beam of α particles was collimated by two 0.24-cm Mo collimators 15 cm apart before entering the target chamber. The α -particle energy was determined by calibrating the energy-analyzing magnet by standard threshold reactions.²⁵ Thin targets were mounted at 45° to

the incident-beam direction. The targets were 30–150 $\mu\text{g}/\text{cm}^2$ thick and were vacuum deposited on 20–50- $\mu\text{g}/\text{cm}^2$ -thick carbon backings. A KeveX Si(Li) detector with a FWHM (full width at half-maximum) resolution of 172 eV at 5.898 keV was positioned outside the target chamber 5.0 cm from the target and at an angle of 90° to the incident-beam direction. Hence, x rays from the target were required to pass through a 0.025 cm Mylar chamber window, 5.0 cm of air, and 0.0025 cm Be detector window. A typical x-ray spectrum is shown in Fig. 1 for the K_α and K_β x rays of Ni. The absolute efficiency of this detector system was measured using standard calibrated radioactive sources of ^{57}Co , ^{65}Zn , ^{51}Cr , ^{54}Mn , and ^{241}Am following well-defined procedures.^{26–28} The sources were mounted in the chamber at the target location and therefore had a geometry representative of the actual experimental conditions. The absolute efficiency includes the intrinsic efficiency and fractional solid angle intercepted by the Si(Li) detector as well as x-ray attenuation by the Mylar, air, and Be. The use of a number of independently calibrated radioactive sources with overlapping x- and γ -ray energies gives one good confidence in the overall normalization of the experimental data. The measured efficiency curve is shown in Fig. 2.

A Si surface-barrier detector mounted at 150° with respect to the incident-beam direction was used to detect incident α particles which were Rutherford scattered by the target material and carbon backing. A typical Rutherford spectrum for α particles scattered from a Ni target and the C backing is shown in Fig. 1. The solid angle of the Rutherford detector was measured using a calibrated radioactive ^{244}Cm α -particle source. The measured solid angle of the Si surface-barrier detector was 2.6×10^{-4} sr.

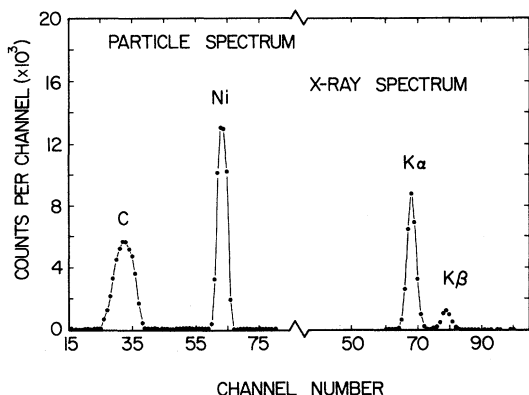


FIG. 1. Typical x-ray and charged-particle spectra produced by α -particle bombardment of a thin Ni foil.

III. DATA ANALYSIS

The number of detected K x rays is given by the expression

$$N_x = \sigma_x (In) \Sigma_x,$$

where σ_x is the x-ray production cross section, In is the product of incident projectile flux and the number of target nuclei, and Σ_x is the absolute efficiency of the detector system and includes the intrinsic efficiency of the detector, the fractional solid angle subtended by the detector at the target, and the x-ray attenuation in the Mylar and Be windows and the 5.0 cm air space.

The number of α particles which are detected in the particle detector is given by

$$N_R = \sigma_R(\theta)(In)\Omega_R,$$

where $\sigma_R(\theta)$ is the Rutherford differential elastic scattering cross section in the laboratory frame of reference at the scattering angle θ and Ω_R is the solid angle subtended by the particle detector at the target.

By accumulating the x-ray and particle spectra simultaneously, the incident-beam flux and the number of target nuclei may be cancelled out of the ratio N_x/N_R resulting in the expression

$$\frac{N_x}{N_R} = \frac{\sigma_x \Sigma_x}{\sigma_R(\theta)\Omega_R}.$$

The x-ray production cross section is given by

$$\sigma_x = \sigma_R(\theta) \frac{\Omega_R}{N_R} \left[\frac{N_{x\alpha}}{\Sigma_{x\alpha}} + \frac{N_{x\beta}}{\Sigma_{x\beta}} \right],$$

where the numbers of $K\alpha$ and $K\beta$ x rays have been divided by their respective efficiencies. Inherent in this expression for the x-ray production cross section are two assumptions: (i) the charged-particle-induced emission of characteristic x rays is isotropic and (ii) the α particles detected at $\theta = 150^\circ$ are truly Rutherford scattered. The isotropy of charged-particle-induced x-ray emission has been experimentally confirmed by a number of

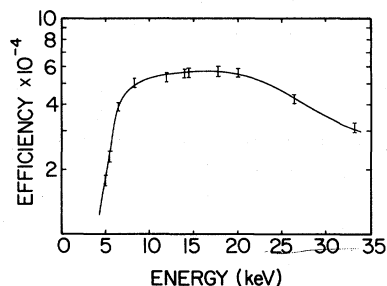


FIG. 2. Measured absolute efficiency of the x-ray detector system.

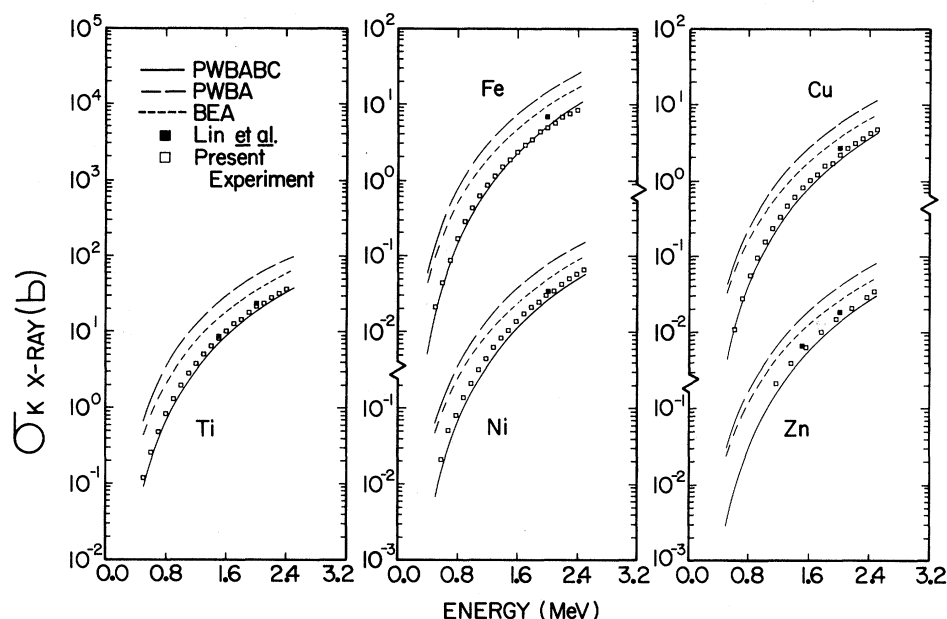


FIG. 3. Present experimental x-ray-production cross sections are compared to the results of Lin *et al.* (Ref. 2). The curves are theoretical calculations of the BEA, PWBA, and PWBA with binding energy and Coulomb deflection corrections.

authors at least for x rays from the *K* and *L* shells.²⁹⁻³¹ The Rutherford nature of the yield of particles scattered elastically at extreme back angles has been confirmed experimentally at this laboratory by Lear and Gray.⁸

The deadtime in the counting electronics was maintained at 5% or less. The yields in the x-ray and Rutherford detectors reflect the deadtime corrections.

IV. RESULTS AND DISCUSSION

The present experimental x-ray production cross sections are compared to the earlier results of Lin, Duggan, and Carlton^{2,14} in Fig. 3. The relative uncertainties in the present results are smaller than the size of the data points. Relative uncertainties are those which vary with projectile energy and do not include any normalization uncertainties. The sources of uncertainty are given in Table I. The agreement found between the energy dependences of the two sets of cross-section data is very good and in all cases the normalizations of the data are within experimental uncertainties. The total uncertainties in the data of Lin, Duggan, and Carlton^{2,14} are $\pm 30\%$ for Ti, Fe, and Cu, and $\pm 50\%$ for Zn and Ni. The x-ray production cross sections determined in the present experiment are given in Table II and have total uncertainties $\leq 9\%$. For those data which had an observable energy loss as determined from the FWHM width of the Rutherford-scattered peak, the incident-particle energy at the center of the target foil is given.

The theoretical curves shown in Fig. 3 were

calculated using the computer code, XCODE.³² In making comparisons with experiment, theoretical x-ray production cross sections were obtained using the fluorescence yields taken from Bambynek *et al.*,³³ as calculated by McGuire.³⁴ The calculations include the BEA,²⁰⁻²² the PWBA,^{17,18} and the PWBA corrected for Coulomb deflection (CD) of the incident projectile and for increased electron binding energy (BE), PWBABC.^{19,23} The general

TABLE I. Sources of uncertainty in the measured cross sections.

Source	Range
Relative uncertainty	
Counting statistics and background subtraction	
K_{α} and K_{β} x-ray yields	1-4%
Back-scattered α -particle yields	1-2%
Relative uncertainty	< 4.5%
Normalization uncertainty	
Absolute efficiency calibration	
Source strength	3% ^a
Source x-ray yields	1-2%
Source relative photon intensities	< 3% ^b
Particle detector solid angle	< 3%
Rutherford differential cross section through	
uncertainty in angle θ of particle detector	< 4%
Normalization uncertainty	< 7.1%
Total uncertainty ^c	< 9%

^aReference 8.

^bReference 26-28.

^cThe total uncertainty is the square root of the sum of the squares of the individual uncertainties.

TABLE II. *K*-shell experimental x-ray production cross sections for α -particle bombardment.

Element	Z	Energy (MeV)	σ_x^a (b)	Element	Z	Energy (MeV)	σ_x^a (b)
Ti	22	0.50	0.121	Fe	26	0.50	0.021
		0.60	0.261			0.60	0.044
		0.70	0.491			0.70	0.087
		0.80	0.848			0.80	0.169
		0.90	1.33			0.90	0.282
		1.00	2.00			1.00	0.428
		1.10	2.87			1.10	0.617
		1.20	3.83			1.20	0.845
		1.30	5.15			1.30	1.13
		1.40	6.57			1.40	1.49
		1.50	8.42			1.50	1.86
		1.60	10.3			1.60	2.32
		1.70	12.9			1.70	2.87
		1.80	14.7			1.80	3.42
		1.90	18.2			1.90	4.32
		2.00	21.7			2.00	4.89
		2.10	24.0			2.10	5.74
2.20	28.5	2.20	6.74				
2.30	32.2	2.30	7.50				
2.40	37.0	2.40	8.44				
V	23	0.50	0.074	Ni	28	0.57	0.021
		0.60	0.181			0.67	0.051
		0.70	0.336			0.77	0.081
		0.80	0.583			0.87	0.138
		0.90	0.947			0.97	0.211
		1.00	1.39			1.07	0.321
		1.10	2.07			1.17	0.449
		1.20	2.69			1.28	0.634
		1.30	3.66			1.38	0.835
		1.40	4.90			1.48	1.07
		1.50	6.02			1.58	1.39
		1.60	7.59			1.68	1.73
		1.70	9.34			1.78	2.10
		1.80	11.3			1.88	2.52
		1.90	13.7			1.98	3.03
		2.00	16.2			2.08	3.58
		2.10	19.0			2.18	4.29
2.20	21.3	2.28	5.06				
2.30	26.0	2.38	5.83				
2.40	28.7	2.48	6.62				
Cr	24	0.50	0.053	Cu	29	0.60	0.011
		0.60	0.125			0.70	0.028
		0.70	0.238			0.80	0.057
		0.80	0.425			0.90	0.097
		0.90	0.661			1.00	0.157
		1.00	1.03			1.10	0.234
		1.10	1.45			1.20	0.333
		1.20	1.96			1.30	0.468
		1.30	2.67			1.40	0.612
		1.40	3.51			1.50	0.816
		1.50	4.24			1.60	1.02
		1.60	5.24			1.70	1.22
		1.70	6.97			1.80	1.59
		1.80	8.28			1.90	1.71
		1.90	9.92			2.00	2.22
		2.00	11.5			2.10	2.69
		2.10	13.5			2.20	3.12
2.20	15.8	2.30	3.60				
2.30	18.3	2.40	4.25				
2.40	19.9	2.50	4.75				

TABLE II (continued)

Element	Z	Energy (MeV)	σ_x^a (b)	Element	Z	Energy (MeV)	σ_x^a (b)		
Zn	30	1.16	0.217	Rb	37	1.57	0.073		
		1.36	0.403			1.77	0.121		
		1.55	0.660			1.97	0.183		
		1.76	1.03			2.17	0.261		
		1.96	1.54			2.37	0.384		
		2.16	2.12			Sr	38	1.00	0.0045
		2.36	2.96					1.20	0.014
		2.46	3.55					1.40	0.036
Ga	31	1.29	0.203	1.60	0.077				
		1.49	0.366	1.80	0.108				
		1.69	0.611	2.00	0.164				
		1.90	0.941	2.10	0.190				
		2.10	1.36	2.20	0.249				
		2.30	1.91	2.40	0.319				
		2.41	2.21	2.50	0.360				
		As	33	1.36	0.113	Y	39	0.87	0.0022
1.57	0.221			0.97	0.0039				
1.77	0.354			1.07	0.0070				
1.87	0.462			1.17	0.011				
1.97	0.576			1.27	0.016				
2.07	0.678			1.37	0.023				
2.17	0.866			1.47	0.034				
2.37	1.19			1.57	0.042				
Se	34	2.47	1.40	1.67	0.057				
		1.18	0.061	1.77	0.074				
		1.37	0.113	1.88	0.090				
		1.58	0.192	1.98	0.113				
		1.78	0.304	2.08	0.131				
		1.98	0.495	2.18	0.162				
		Rb	37	1.17	0.020	2.28	0.186		
				1.37	0.038	2.38	0.224		
				2.48	0.264				

^aUncertainties in these data are given in Table I. The total uncertainty is $\leq 9\%$.

shape of the data is reproduced by all of the theories shown.

The PWBA, which has met with reasonably good success in describing the interactions of light incident ions with target electrons at energies above a few MeV,^{2,19} consistently overpredicts the measured cross sections at low energies.^{2,19} This is very evident for all elements investigated and is shown in Fig. 3 for typical results.

The BEA provides better agreement than the PWBA with experimental results but still overpredicts the cross sections by 70%. The CBEA of Hansen³⁵ in configuration space with inclusion of approximate relativistic corrections to the electron's velocity distribution is not shown since the results are very little different from the BEA for the energy region of interest.

The PWBABC provides the best agreement with the experimental cross sections. The CD and BE

corrections overcorrect the experimental data in all cases except for some of the very-low-energy data points. The PWBA corrected for BE (PWBAB) and CD (PWBAC) separately are shown in Fig. 4 for Y and V. For V, the BE correction is much larger than the CD correction at all energies investigated. For Y, the CD correction is much more important, as expected, especially for smaller projectile energies. Here the CD correction exceeds the BE correction in magnitude.

While the corrections to the PWBA improve the agreement between theory and the smoothly varying magnitude of the experimental cross sections as exhibited here for the K shell and also for the L shell,³⁶ it actually reduces the agreement with the structure in the L shell as indicated by the ratios of partial cross sections, $L\alpha/L\gamma_{2,3}$.³⁶ The disagreement increases with increasing Z_1 of the incident projectile.³⁶

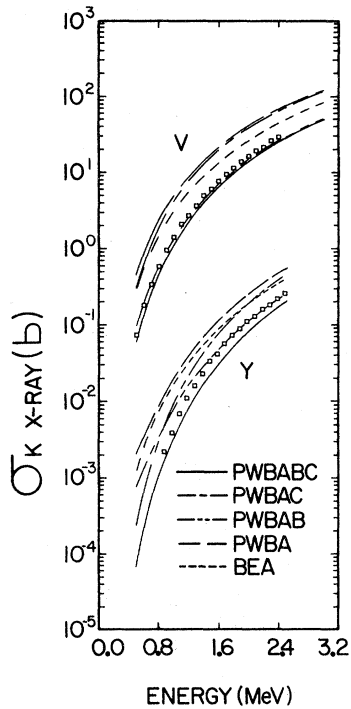


FIG. 4. Experimental x-ray-production cross sections of V and Y are shown with the theoretical predictions of BEA, PWBA, PWBA with binding energy (BE) correction, PWBA with Coulomb deflection (CD) correction, and PWBA with BE and CD corrections.

It has been noted by Choi³⁷ that employing relativistic-electron wave functions for medium-heavy and heavy elements in the large-energy-transfer region can raise the theoretical cross-section predictions. Whether the use of relativistic-electron wave functions will improve the agreement between theory and experiment for the elements considered in this paper is yet to be determined. It is not clear that relativistic corrections should be applied as an *ad hoc* correction on top of the BE and CD corrections because of the effect the relativistic description may have on the magnitudes of the BE and CD corrections.

In addition to the experimental cross sections, we have extracted $K\beta/K\alpha$ ratios for a comparison with the calculated values of Scofield³⁸ and with $K\beta/K\alpha$ ratios determined from proton-induced-ionization experiments.^{8,13} This comparison is made in Table III. The experimental $K\beta/K\alpha$ values given are weighted averages of the $K\beta/K\alpha$ values determined at each energy and are corrected for the different efficiencies for the $K\alpha$ and $K\beta$ lines. The uncertainties given include counting statistics (1–4%) and background subtraction (2–3%), and in most cases are less than 5%. The agreement between experiment and theory is very good in most cases with the theoretical values an average of 6% larger than the experimental values. The agreement between $K\beta/K\alpha$ ratios determined for proton-induced ionization and α -particle-induced

TABLE III. $K\beta/K\alpha$ ratios.

Element	Z	Present experiment ^a (α -particle projectile)	$K\beta/K\alpha$	
			Theory ^b	Previous work (proton projectile)
Ti	22	0.121 ± 0.016	0.136	
V	23	0.128 ± 0.006	0.137	
Cr	24	0.124 ± 0.006	0.134	
Fe	26	0.129 ± 0.006	0.139	0.139 ± 0.004 ^c
Ni	28	0.137 ± 0.007	0.140	
Cu	29	0.133 ± 0.007	0.138	0.145 ± 0.004 ^c
Zn	30	0.139 ± 0.007	0.141	0.146 ± 0.004 ^c
Ga	31	0.142 ± 0.007		0.155 ± 0.004 ^c
As	33	0.152 ± 0.008	0.156	0.153 ± 0.004 ^c
Se	34	0.152 ± 0.010	0.162	0.162 ± 0.015 ^d
Rb	37	0.165 ± 0.010	0.178	0.175 ± 0.014 ^d
Sr	38	0.176 ± 0.009	0.183	0.199 ± 0.016 ^d
Y	39	0.183 ± 0.009		0.181 ± 0.015 ^d

^a Weighted averages of $K\beta/K\alpha$ values determined at each energy. Uncertainties include counting statistics and background subtraction.

^b Values given in Ref. 38.

^c Values given in Ref. 8.

^d Values given in Ref. 13.

ionization is very good.

Li *et al.*³⁹ and Kauffman *et al.*⁴⁰ have observed energy shifts for *K* x rays for α -particle bombardment due to simultaneous excitation of the *L* shell. The fraction of the number of *K* x rays emitted in the presence of an *L*-shell vacancy has been shown to increase with decreasing target atomic number.³⁹ For Ti, which has the lowest atomic number investigated, a calculation of the magnitude of an energy shift due to multiple ionization is ~ 7 eV even if one assumes that 20–25% of the *K* x rays^{39,40} were emitted in the presence of an *L*-shell vacancy. The present experiment

was not designed to measure energy shifts of this magnitude.

ACKNOWLEDGMENTS

The authors would like to thank G. M. Light for assistance with some of the data acquisition and J. Rowe and S. Wilson for help with the data analysis. We would especially like to express our appreciation to G. Pepper for the use of the computer code, XCODE, and to the Computer Center at North Texas State Univ. for providing the computer time necessary for the lengthy theoretical calculations.

*This work supported in part by the Faculty Research Fund, NTSU and by the Robert A. Welch Foundation.

¹J. D. Garcia, R. J. Fortner, and T. M. Kavanagh, *Rev. Mod. Phys.* **45**, 111 (1973).

²J. Lin, J. L. Duggan, and R. F. Carlton, in *Proceedings of the International Conference on Inner-Shell Ionization Phenomena and Future Applications, Atlanta, Georgia, 1972*, edited by R. W. Fink, S. T. Manson, J. M. Palms, and P. V. Rao, CONF-720404 (U. S. AEC, Oak Ridge, Tenn., 1973), p. 998.

³C. H. Rutledge and R. L. Watson, *At. Data Nucl. Data Tables* **12**, 195 (1973).

⁴T. J. Gray, R. Lear, R. J. Dexter, F. N. Schwettmann, and K. C. Wiemer, *Thin Solid Films* **19**, 103 (1973).

⁵J. L. Duggan, W. L. Beck, L. Albrecht, L. Munz, and J. D. Spaulding, in *Advances in X-Ray Analysis*, edited by K. F. J. Heinrich, C. S. Barrett, J. B. Newkirk, and C. O. Ruud (Plenum, New York, 1972), Vol. 15, p. 407.

⁶T. B. Johansson, R. Akselsson, and S. A. E. Johansson, *Nucl. Instr. Methods* **84**, 141 (1970).

⁷T. B. Johansson, R. Akselsson, and S. A. E. Johansson, in Ref. 5, Vol. 15, p. 373.

⁸R. Lear and T. J. Gray, *Phys. Rev. A* **8**, 2469 (1973).

⁹R. Akselsson and T. B. Johansson, *Z. Phys.* **266**, 245 (1974).

¹⁰J. M. Hansteen and S. Messelt, *Nucl. Phys.* **2**, 526 (1957).

¹¹S. Datz, J. L. Duggan, L. C. Feldman, E. Laegsgaard, and J. U. Anderson, *Phys. Rev. A* **9**, 192 (1974).

¹²F. Abrath and T. J. Gray, *Phys. Rev. A* **9**, 682 (1974).

¹³T. L. Criswell and T. J. Gray, *Phys. Rev. A* **10**, 1145 (1974).

¹⁴J. Lin, J. L. Duggan, and R. F. Carlton (private communication).

¹⁵W. Brandt, R. Laubert, and I. Sellin, *Phys. Rev.* **151**, 56 (1966).

¹⁶R. L. Watson, C. W. Lewis, and J. B. Natowitz, *Nucl. Phys. A* **154**, 561 (1970).

¹⁷E. Merzbacher and H. Lewis, in *Encyclopedia of Physics*, edited by S. Flugge (Springer-Verlag, Berlin, 1958), Vol. 34, p. 166.

¹⁸G. S. Khandelwal, B.-H. Choi, and E. Merzbacher, *At.*

Data **1**, 103 (1969).

¹⁹W. Brandt, in Ref. 2, p. 948.

²⁰J. D. Garcia, E. Gerjuoy, and J. E. Welker, *Phys. Rev.* **165**, 66 (1968).

²¹J. D. Garcia, *Phys. Rev. A* **1**, 1402 (1970).

²²J. D. Garcia, *Phys. Rev. A* **1**, 280 (1970).

²³G. Basbas, W. Brandt, and R. Laubert, *Phys. Rev. A* **7**, 983 (1973).

²⁴T. J. Gray, Conference on Ion Beam Analysis of Near Surface Regions, June, 1974, Catania, Italy (unpublished).

²⁵J. B. Marion, *Rev. Mod. Phys.* **38**, 660 (1966).

²⁶L. B. Magnusson, *Phys. Rev.* **107**, 161 (1957).

²⁷J. S. Hansen, J. C. McGeorge, D. Nix, W. D. Schmidt-Ott, I. Unus, and R. W. Fink, *Nucl. Instr. Methods* **106**, 365 (1973).

²⁸R. J. Gehrke and R. A. Lokken, *Nucl. Instr. Methods* **97**, 219 (1971).

²⁹E. M. Bernstein and H. W. Lewis, *Phys. Rev.* **95**, 83 (1954).

³⁰L. M. Middleman, R. L. Ford, and R. Hofstadter, *Phys. Rev. A* **2**, 1429 (1970).

³¹C. W. Lewis, R. L. Watson, and J. B. Natowitz, *Phys. Rev. A* **5**, 1773 (1972).

³²G. Pepper, thesis (North Texas State University, 1974) (unpublished).

³³W. Bambynek, B. Crasemann, R. W. Fink, H.-U. Freund, H. Mark, C. D. Swift, R. E. Price, and P. V. Rao, *Rev. Mod. Phys.* **44**, 716 (1972).

³⁴E. J. McGuire, *Phys. Rev. A* **2**, 273 (1970).

³⁵J. S. Hansen, *Phys. Rev. A* **8**, 822 (1973).

³⁶T. J. Gray, in *Proceedings of the Third Conference on the Use of Small Accelerators in Research, Teaching, and Industrial Applications, Denton, Texas, 1974*, edited by J. L. Duggan and I. L. Morgan, CONF-741040 (ERDA, Oak Ridge, Tenn., 1975), Vol. 1.

³⁷B.-H. Choi, *Phys. Rev. A* **4**, 1002 (1971).

³⁸J. H. Scofield, *Phys. Rev. A* **9**, 1041 (1974).

³⁹T. K. Li, R. L. Watson, and J. S. Hansen, *Phys. Rev. A* **8**, 1258 (1973).

⁴⁰R. L. Kauffman, J. H. McGuire, P. Richard, and C. F. Moore, *Phys. Rev. A* **8**, 1233 (1973).